NASA TECHNICAL MEMORANDUM

NASA TM X-3115

NASA TM X-3115

AERODYNAMIC ROLL DAMPING OF A T-TAIL TRANSPORT CONFIGURATION

by Richmond P. Boyden

Langley Research Center
Hampton, Va. 23665

NATIONAL AERONAUTICS AND SPACE ADMINISTRATION • WASHINGTON, D. C. • DECEMBER 1974

1. Report No.	2. Government Accession No.	3. Recipient's Catalog No.
NASA TM X-3115		

4. Title and Subtitle	5. Report Date
AERODYNAMIC ROLL DAMPING OF A T-TAIL TRANSPORT CONFIGURATION	December 1974
	6. Performing Organization Code

7. Author(s)	8. Performing Organization Report No.
Richmond P. Boyden	L-9378
	10. Work Unit No.
	512-53-01-06

9. Performing Organization Name and Address	11. Contract or Grant No.
NASA Langley Research Center Hampton, Va. 23665	
	13. Type of Report and Period Covered
	Technical Memorandum

12. Sponsoring Agency Name and Address	14. Sponsoring Agency Code
National Aeronautics and Space Administration Washington, D.C. 20546	

15. Supplementary Notes

16. Abstract

The aerodynamic roll damping and the yawing moment due to roll rate for a model of a T-tail transport with aft-mounted engines were measured by means of a small-amplitude forced-oscillation mechanism. The tests were made for Mach numbers between 0.21 and 0.80 over a range of angles of attack from about -4° to 22°.

The basic configuration had positive damping in roll at low angles of attack with regions of low positive and negative damping for angles of attack above 8° to 10°. There was good agreement between the theoretical estimates of the roll damping for the wing alone and the experimental results at an angle of attack of 0° for Mach numbers of 0.60 and less.

The T-tail configuration and the engine nacelles mounted aft on the fuselage did not significantly affect either the damping in roll or the yawing moment due to roll rate.

17. Key Words (Suggested by Author(s))	18. Distribution Statement
Dynamic stability Roll damping T-tail transport	Unclassified – Unlimited STAR Category 02

19. Security Classif. (of this report)	20. Security Classif. (of this page)	21. No. of Pages	22. Price*
Unclassified	Unclassified	29	$3.75

*For sale by the National Technical Information Service, Springfield, Virginia 22151

AERODYNAMIC ROLL DAMPING OF A T-TAIL TRANSPORT CONFIGURATION

By Richmond P. Boyden
Langley Research Center

SUMMARY

The aerodynamic roll damping and the yawing moment due to roll rate for a model of a T-tail transport with aft-mounted engines were measured by means of a small-amplitude forced-oscillation mechanism. The tests were made for Mach numbers between 0.21 and 0.80 over a range of angles of attack from about -4° to 22°.

The basic configuration had positive damping in roll at low angles of attack with regions of low positive and negative damping for angles of attack above 8° to 10°. There was good agreement between the theoretical estimates of the roll damping for the wing alone and the experimental results at an angle of attack of 0° for Mach numbers of 0.60 and less.

The T-tail configuration and the engine nacelles mounted aft on the fuselage did not significantly affect either the damping in roll or the yawing moment due to roll rate.

INTRODUCTION

The aerodynamic characteristics of T-tail transport configurations with the jet engines mounted at the rear of the fuselage have been the subject of many investigations over the past few years in connection with the "deep stall" phenomenon. (See refs. 1, 2, 3, and 4.) Most of these studies have focused on the longitudinal aerodynamic characteristics. However, some concern has been expressed over both the lateral-directional handling qualities and the lack of data on the lateral-directional dynamic derivatives of this type of configuration in the stall regime (ref. 5) which could be encountered during flight test or during normal operations because of an inadvertent upset. In order to more fully document the lateral-directional aerodynamic characteristics of the T-tail type of configuration, the National Aeronautics and Space Administration has investigated the roll damping and the yawing moment due to roll rate of a representative configuration. The tests were made at Mach numbers from 0.21 to 0.80 over an angle-of-attack range from approximately -4° to 22°.

SYMBOLS

The aerodynamic parameters in this report are generally referred to the body system of axes as shown in figure 1 in which the coefficients, angles, and angular velocity are shown in the positive sense. These axes originate at the center of moments which was located at 41.4 percent of the wing mean geometric chord. The lift data and the roll damping data taken from references 1 and 2, respectively, are in the stability-axis system.

Most of the measurements were made in U.S. Customary Units and converted to SI Units. Values in this report are presented in the International System of Units (SI) with the U.S. Customary Units given in parentheses. Details on the use of SI together with the physical constants and conversion factors are given in reference 6.

b	reference span, 0.9144 meter (36.00 inches)
$\bar{c}$	mean geometric chord, 0.1314 meter (5.175 inches)
f	frequency of oscillation, hertz
k	reduced-frequency parameter, $\omega b/2V$, radians
M	free-stream Mach number
p	angular velocity of model about X-axis, radians/second
q_∞	free-stream dynamic pressure, pascals (pounds/foot^2)
R	Reynolds number based on $\bar{c}$
S	reference area, 0.1074 meter^2 (1.156 feet^2)
V	free-stream velocity, meters/second (feet/second)
X,Y,Z	reference body axes
α	angle of attack, degrees
β	angle of sideslip, degrees

ω angular velocity, $2\pi f$, radians/second

C_L lift coefficient, Lift/$q_\infty S$

C_l rolling-moment coefficient, Rolling moment/$q_\infty Sb$

C_n yawing-moment coefficient, Yawing moment/$q_\infty Sb$

$C_{l_\beta} = \frac{\partial C_l}{\partial \beta}$ per radian

$C_{l_{\dot\beta}} = \frac{\partial C_l}{\partial\left(\frac{\dot\beta b}{2V}\right)}$ per radian

$C_{l_p} = \frac{\partial C_l}{\partial\left(\frac{pb}{2V}\right)}$ per radian

$C_{l_{\dot p}} = \frac{\partial C_l}{\partial\left(\frac{\dot p b^2}{4V^2}\right)}$ per radian

$C_{l_\beta} \sin\alpha - k^2 C_{l_{\dot p}}$ rolling moment due to roll displacement parameter, per radian

$C_{l_p} + C_{l_{\dot\beta}} \sin\alpha$ damping-in-roll parameter, per radian

$C_{n_\beta} = \frac{\partial C_n}{\partial \beta}$ per radian

$C_{n_{\dot\beta}} = \frac{\partial C_n}{\partial\left(\frac{\dot\beta b}{2V}\right)}$ per radian

$C_{n_p} = \frac{\partial C_n}{\partial\left(\frac{pb}{2V}\right)}$ per radian

$$C_{n_{\dot{p}}} = \frac{\partial C_n}{\partial\left(\frac{\dot{p}b^2}{4V^2}\right)} \text{ per radian}$$

$C_{n_\beta} \sin \alpha - k^2 C_{n_{\dot{p}}}$ yawing moment due to roll displacement parameter, per radian

$C_{n_p} + C_{n_{\dot{\beta}}} \sin \alpha$ yawing moment due to roll rate parameter, per radian

A dot over a quantity indicates a first derivative with respect to time.

Model component designations:

B body

H horizontal tail

N engine nacelles

V vertical tail

W wing

APPARATUS

Model

The model used for this investigation was a scaled-down version (0.7759 scale) of the model used in references 1 and 2. Only one modification to the model lines was required for the present investigation: the aft portion of the fuselage was enlarged to allow for clearance for the sting. The model was constructed from magnesium, except for the forward fuselage section which was fiberglass, in order to keep the moments of inertia low enough to be compatible with the forced-oscillation balance. A steel balance adapter was used to provide a solid mounting surface and to carry the aerodynamic and inertial loads. The model was fabricated so that the wing, horizontal tail, and engine nacelles could be removed for a component breakdown test. A drawing of the model is presented in figure 2 and a photograph of the model mounted on the forced-oscillation roll mechanism is presented in figure 3.

Forced-Oscillation Mechanism

A sketch of the small-amplitude oscillatory-roll mechanism used for this investigation is shown in figure 4. The basic principles of operation of the oscillatory-roll mechanism are the same as those for the small-amplitude rigidly forced-oscillation pitch and yaw system of reference 7. A 1500-W (2 hp) electric motor with an eccentric drive oscillates the sting and model in an essentially sinusoidal motion. The model is rigidly forced in a fixed 2.5° amplitude oscillation about the sting axis (body X-axis) at a variable frequency. A mechanical torsion spring internal to the sting is attached to the front of the strain-gage balance to permit the model to be oscillated at the frequency for velocity resonance whereby the mechanical torsion spring, plus any aerodynamic spring, balances the model inertia. The only torque then required to oscillate the model at that particular frequency is equal to the torque due to the aerodynamic damping (ref. 7).

Although the models may be oscillated at frequencies from about 1 to 30 hertz, the damping torque is obtained most accurately by operating at the frequency for velocity resonance. The rolling- and yawing-moment strain gages are located forward of all the bearings and other friction-producing devices. A strain-gage bridge is mounted on the mechanical torsion spring to provide a signal proportional to the model angular displacement in roll.

Wind Tunnel

This investigation was made in the Langley high-speed 7- by 10-foot tunnel. This single-return, atmospheric, continuous-flow facility had a closed test section during this series of tests and was capable of operation at Mach numbers from low subsonic to in excess of 0.90. Additional information on the tunnel and its operating conditions is contained in reference 8. The sting support system when used with the forced-oscillation roll mechanism (figs. 3 and 4) provided an angle-of-attack range from about -4° to 22°.

MEASUREMENTS

Measurements were made of the amplitude of the torque required to oscillate the model in roll T_X, the amplitude of the angular displacement in roll of the model with respect to the fixed portion of the sting Φ, the phase angle σ between T_X and Φ, and the angular velocity of the forced oscillation ω. The viscous damping coefficient in roll C_X for this single-degree-of-freedom system was computed as

$$C_X = \frac{T_X \sin \sigma}{\omega \Phi} \tag{1}$$

and the spring-inertia parameter in roll was computed as

$$K_X - I_X\omega^2 = \frac{T_X \cos \sigma}{\Phi} \tag{2}$$

where K_X is the torsional spring coefficient of the system and I_X is the moment of inertia of the system about the body X-axis.

For this investigation, the damping-in-roll parameter was computed as

$$C_{l_p} + C_{l_{\dot\beta}} \sin \alpha = -\frac{2V}{q_\infty Sb^2}\left[(C_X)_{\text{wind on}} - (C_X)_{\text{wind off}}\right] \tag{3}$$

and the rolling moment due to roll displacement parameter as

$$C_{l_\beta} \sin \alpha - k^2 C_{l_{\dot p}} = -\frac{1}{q_\infty Sb}\left[\left(K_X - I_X\omega^2\right)_{\text{wind on}} - \left(K_X - I_X\omega^2\right)_{\text{wind off}}\right] \tag{4}$$

The wind-off value of C_X is determined at the frequency of wind-off velocity resonance, where the mechanical spring balances the model inertia, since the wind-off value of C_X is independent of frequency and can be determined most accurately at the frequency of velocity resonance. The wind-on and wind-off values of $K_X - I_X\omega^2$ are determined at the same frequency since $K_X - I_X\omega^2$ is a function of frequency.

As part of the rolling oscillation test, measurements were made of the amplitude of the yawing torque T_Z induced by the rolling oscillation and the phase angle ϵ between T_Z and the rolling displacement Φ. The yawing-moment coefficient in phase with rolling velocity for this system was

$$C_{n,X} = \frac{T_Z \sin \epsilon}{\omega\Phi} \tag{5}$$

and the yawing-moment parameter in phase with rolling displacement was

$$B + I_{XZ}\omega^2 = \frac{T_Z \cos \epsilon}{\Phi} \tag{6}$$

where B is the torsional spring coefficient in yaw induced by a roll displacement and I_{XZ} is the product of inertia of the system.

For these tests, the yawing moment due to roll rate parameter was computed as

$$C_{n_p} + C_{n_{\dot{\beta}}} \sin \alpha = -\frac{2V}{q_\infty Sb^2}\left[\left(C_{n,X}\right)_{\text{wind on}} - \left(C_{n,X}\right)_{\text{wind off}}\right] \tag{7}$$

and the yawing moment due to roll displacement parameter was computed as

$$C_{n_\beta} \sin \alpha - k^2 C_{n_{\dot{p}}} = -\frac{1}{q_\infty Sb}\left[\left(B + I_{XZ}\omega^2\right)_{\text{wind on}} - \left(B + I_{XZ}\omega^2\right)_{\text{wind off}}\right] \tag{8}$$

The wind-off and the wind-on values of $B + I_{XZ}\omega^2$ are determined at the same frequency since $B + I_{XZ}\omega^2$ is a function of frequency.

It should be emphasized that the measurement of the primary damping parameter $C_{l_p} + C_{l_{\dot{\beta}}} \sin \alpha$, where the system is operated at the frequency for velocity resonance so that the component of torque in phase with displacement is zero, is inherently more accurate than the measurement of the secondary damping parameter $C_{n_p} + C_{n_{\dot{\beta}}} \sin \alpha$, where the damping parameters are measured in the presence of large moments in phase with displacement.

TESTS

The dynamic stability parameters were obtained at Mach numbers of 0.21, 0.30, 0.40, 0.60, and 0.80 over an angle-of-attack range which varied depending on the specific configuration and Mach number. At Mach numbers of 0.21, 0.30, and 0.40, all the configurations were tested over the entire available angle-of-attack range from about -4° to 22°, but for Mach numbers of 0.60 and 0.80 the upper limit on angle of attack was restricted by an unwanted vibration of the model-sting combination in the pitch plane and by the balance load limits. Nominal test conditions are listed in the following table:

Mach number	Dynamic pressure		Reynolds number
	Pa	lb/ft^2	
0.21	3 036	63.4	0.59×10^6
.30	5 990	125.1	.82
.40	10 179	212.6	1.05
.60	20 067	419.1	1.42
.80	29 825	622.9	1.61

The amplitude of the roll oscillation was about 2.5° and was determined by the mechanical throw of the actuating crank. The range of the reduced-frequency parameter was from 0.059 to 0.363.

In order to insure a turbulent boundary layer over the model, carborundum grains were applied as three-dimensional roughness to the model components. This roughness consisted of transition strips 1.27 cm (0.50 in.) behind the leading edge of the wing on both the upper and lower surfaces and a band around the fuselage 2.54 cm (1.00 in.) behind the fuselage nose. In addition, transition strips were applied to the vertical and horizontal tails 0.76 cm (0.30 in.) behind the leading edges and in a band around the engine nacelles 1.27 cm (0.50 in.) behind the leading edges. The locations of the transition strips and the grit size (No. 90) were determined by the methods described in reference 9.

RESULTS AND DISCUSSION

Rolling Characteristics

The effects of the basic configuration and variations in this configuration (removal of various components) on the damping-in-roll parameter $C_{l_p} + C_{l_{\dot{\beta}}} \sin \alpha$ and the rolling moment due to roll parameter $C_{l_\beta} \sin \alpha - k^2 C_{l_{\dot{p}}}$ are shown in figure 5.

The damping in roll for the basic configuration BVWNH is positive (negative values of $C_{l_p} + C_{l_{\dot{\beta}}} \sin \alpha$) at low angles of attack over the range of Mach numbers. There is a large decrease in the roll damping for the basic configuration at angles of attack above 4° for Mach numbers of 0.60 and below with the exception of a slight "hook" in the damping parameter at angles of attack between about 6° and 8° for Mach numbers of 0.21, 0.30, and 0.40. The roll damping parameter has zero or positive values (negative roll damping) at an angle of attack of approximately 10° for Mach numbers of 0.21, 0.30, and 0.40 and at an angle of attack of about 8° for a Mach number of 0.60. The variation in roll damping with angle of attack can be related to the local slope of the lift curve; references 1 and 2 show that this basic configuration has a region of approximately zero lift curve slope which begins at about the angle of attack where zero values were found for the roll damping parameter. The lift characteristics of several of the configurations as taken from reference 1 are shown in figure 6 for comparison. For a Mach number of 0.80, the level of the roll damping of the basic configuration BVWNH, as shown in figure 5(e), is highly dependent on the angle of attack and measured values range from about -0.30 to -0.50 at angles of attack between -4° and 8°. The trends in the results for a Mach number of 0.80 are not similar to those for the lower Mach numbers. A shock separation occurring on

the wing might account for this sensitivity of the damping in roll to angle of attack for a Mach number of 0.80. While there are indications of some nonlinearity in the static lift and pitching-moment data for a Mach number of 0.80 over this angle-of-attack range (see ref. 1), not enough data are available to draw a definite conclusion.

Throughout the range of angle of attack and Mach number, the damping-in-roll results for both the configuration with the horizontal tail removed BVWN and the configuration with the engine nacelles removed BVWH are virtually the same as those for the basic configuration. For the configuration with the wing removed BVNH, the damping-in-roll parameter ranges from about -0.02 to -0.03 and is almost completely independent of Mach number and angle of attack. This small roll damping contribution is assumed to be the result of the isolated vertical and horizontal tail assembly, that is, the damping of the tail assembly without the influence of the wing wake.

The results for the component of rolling moment due to roll displacement $C_{l_\beta} \sin \alpha - k^2 C_{l_{\dot{p}}}$ are shown in figure 5. Ideally, under the usual assumption that $C_{l_{\dot{p}}}$ is negligible, the rolling moment due to roll displacement parameter should have a zero value at $\alpha = 0^\circ$. The reason for the small offset apparent in the results for this parameter at $\alpha = 0^\circ$ is not understood, but the amount of offset is not considered significant.

Yawing Characteristics

Figure 7 contains the results concerning the effects of the various configurations that were tested on the yawing moment due to roll rate parameter $C_{n_p} + C_{n_{\dot{\beta}}} \cos \alpha$ and the yawing moment due to roll displacement parameter $C_{n_\beta} \sin \alpha - k^2 C_{n_{\dot{p}}}$.

For the basic configuration BVWNH, the yawing moment due to roll rate parameter becomes increasingly negative at angles of attack between about -2° and about 4° for Mach numbers of 0.60 and less. At still higher angles of attack the values of this parameter rapidly become positive and peak at angles of attack between about 8° and 10°. Above these angles of attack there are additional large variations in this parameter.

The wing was the primary component responsible for the yawing moment due to roll rate since the parameters for all the configurations which included the wing followed the same basic trends with angle of attack for each Mach number.

For the configuration with the wing removed BVNH, the results for $C_{n_p} + C_{n_{\dot{\beta}}} \cos \alpha$ show positive values which decrease in magnitude with an increase in angle of attack for all test Mach numbers. These positive values are believed to be due to the vertical tail.

The results for yawing moment due to roll displacement parameter $C_{n_\beta} \sin \alpha - k^2 C_{n_{\dot{p}}}$ are included in figure 7. This parameter has a $\sin \alpha$ multiplier on

the first term as does the rolling moment due to roll displacement parameter because the roll displacement about the model body axis results in an angle of sideslip. However, with the normal assumption that $C_{n_{\dot{p}}}$ is negligible, the yawing moment due to roll displacement results do indicate that the basic configuration has positive C_{n_β} through the angle-of-attack range and that the addition of the horizontal tail increases the directional stability. Such an increase should be the result of endplating the vertical tail.

Comparison of Experimental Roll Damping Techniques

Figure 8 shows the results of the roll damping tests at $M = 0.30$ in the present investigation and those from reference 2 which used the steady-state forced roll technique on the same model. The stability-axis results for the roll damping obtained by the steady-state forced roll technique can be compared directly with the body-axis results obtained by the forced-oscillation roll technique only at $\alpha = 0^\circ$, because all the required derivatives are not available for an axis transformation and because of the problem in separating the derivatives in the parameter $C_{l_p} + C_{l_{\dot{\beta}}} \sin \alpha$. However, there was good agreement in the values of the roll damping for $\alpha = 0^\circ$ and in the general trends for the various angles of attack.

Comparison of Theoretical Estimates With Experimental Results

Theoretical estimates of the damping-in-roll derivative C_{l_p} for the wing planform of this configuration were computed by using the modified Multhopp lifting-surface theory of reference 10. The theoretical estimates are the potential flow results for a zero thickness planform and are shown in figure 9 for a Mach range from 0 to 0.8. These estimates can be compared with the averaged $\alpha = 0^\circ$ experimental results for the basic configuration BVWNH and the other configurations resulting from removal of different components. The experimental results are for the damping-in-roll parameter $C_{l_p} + C_{l_{\dot{\beta}}} \sin \alpha$ at $\alpha = 0^\circ$ and can be compared with estimates of C_{l_p} because the contribution of the second term $C_{l_{\dot{\beta}}} \sin \alpha$ is zero. The agreement between the experimental results for all the winged configurations and the theoretical estimates for the wing alone is good except at $M = 0.8$. As was seen in figure 5(e), the $M = 0.8$ experimental results were very sensitive to angle of attack, and if the peak negative values of the damping-in-roll parameter at $\alpha = 2^\circ$ had been used in figure 9 instead of the $\alpha = 0^\circ$ values, the agreement of the experimental results with the theoretical estimates would have been much improved.

CONCLUDING REMARKS

The aerodynamic roll damping and the yawing moment due to roll rate for a model of a T-tail transport with aft-mounted engines were measured by means of a small-amplitude forced-oscillation mechanism. The tests were made for Mach numbers between 0.21 and 0.80 over a range of angles of attack from about -4° to 22°.

The basic configuration had positive damping in roll at low angles of attack with regions of low positive and negative damping for angles of attack above 8° to 10°. Good agreement was obtained between the theoretical estimates of the roll damping for the wing alone and the experimental results at an angle of attack of 0° for Mach numbers of 0.60 and less.

The T-tail configuration and the engine nacelles mounted aft on the fuselage did not significantly affect either the damping in roll or the yawing moment due to roll rate.

Langley Research Center,
National Aeronautics and Space Administration,
Hampton, Va., November 5, 1974.

REFERENCES

1. Ray, Edward J.; and Taylor, Robert T.: Effect of Configuration Variables on the Subsonic Longitudinal Stability Characteristics of a High-Tail Transport Configuration. NASA TM X-1165, 1965.

2. Ray, Edward J.: Effect of Large Sideslip Angles on Stability Characteristics of a T-Tail Transport Configuration. NASA TM X-1665, 1968.

3. Lina, Lindsay J.; and Moul, Martin T.: A Simulator Study of T-Tail Aircraft in Deep Stall Conditions. AIAA Paper No. 65-781, 1965.

4. Powers, Bruce G.: A Parametric Study of Factors Influencing the Deep-Stall Pitch-Up Characteristics of T-Tail Transport Aircraft. NASA TN D-3370, 1966.

5. White, Maurice D.; and Cooper, George E.: A Piloted Simulation Study of Operational Aspects of the Stall Pitch-Up. NASA TN D-4071, 1967.

6. Mechtly, E. A.: The International System of Units – Physical Constants and Conversion Factors (Second Revision). NASA SP-7012, 1973.

7. Braslow, Albert L.; Wiley, Harleth G.; and Lee, Cullen Q.: A Rigidly Forced Oscillation System for Measuring Dynamic-Stability Parameters in Transonic and Supersonic Wind Tunnels. NASA TN D-1231, 1962.

8. Schaefer, William T., Jr.: Characteristics of Major Active Wind Tunnels at the Langley Research Center. NASA TM X-1130, 1965.

9. Braslow, Albert L.; and Knox, Eugene C.: Simplified Method for Determination of Critical Height of Distributed Roughness Particles for Boundary-Layer Transition at Mach Numbers From 0 to 5. NACA TN 4363, 1958.

10. Lamar, John E.: A Modified Multhopp Approach for Predicting Lifting Pressures and Camber Shape for Composite Planforms in Subsonic Flow. NASA TN D-4427, 1968.

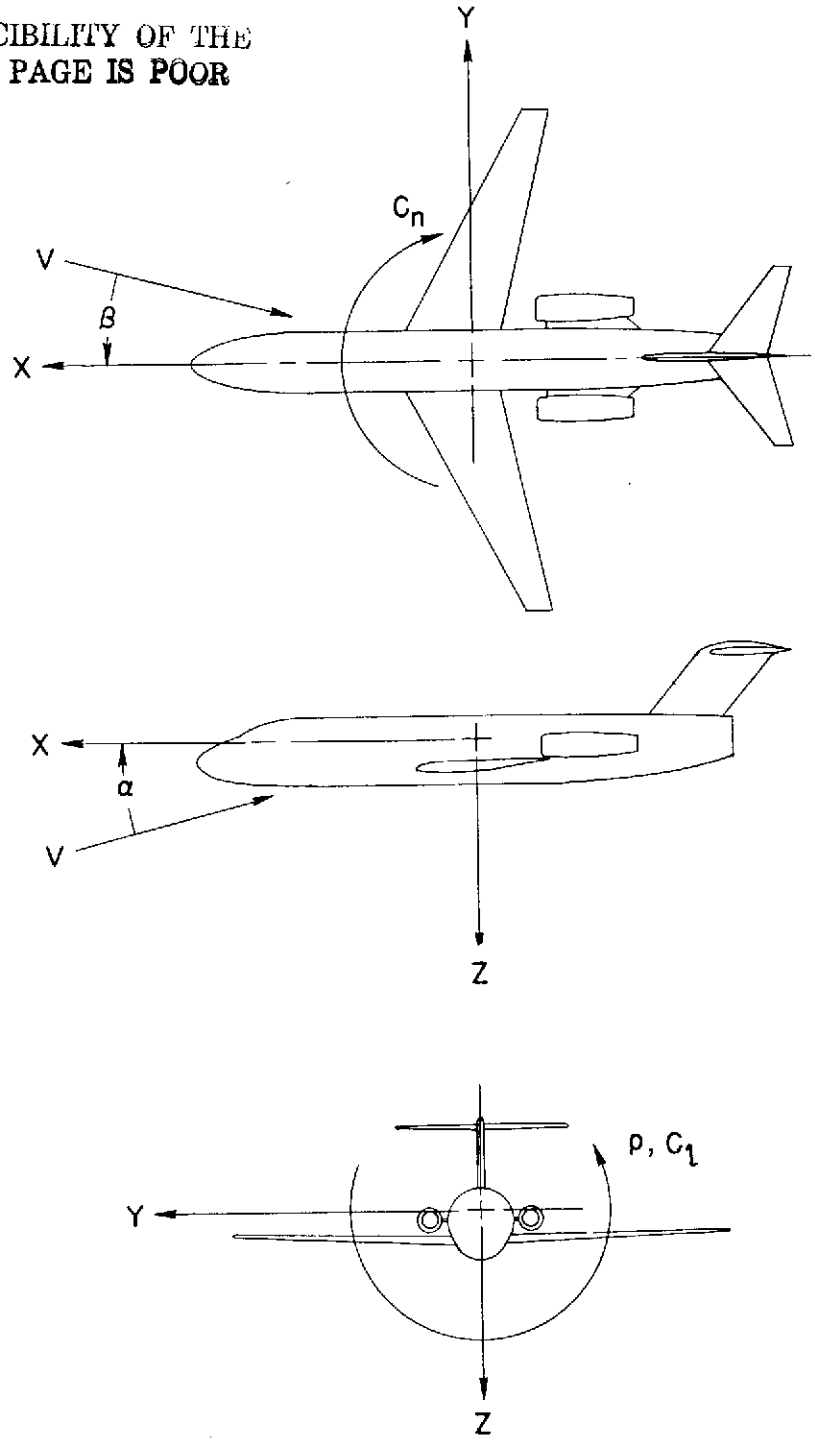

Figure 1.- Body system of axes with coefficients, angles, and angular velocity shown in the positive sense.

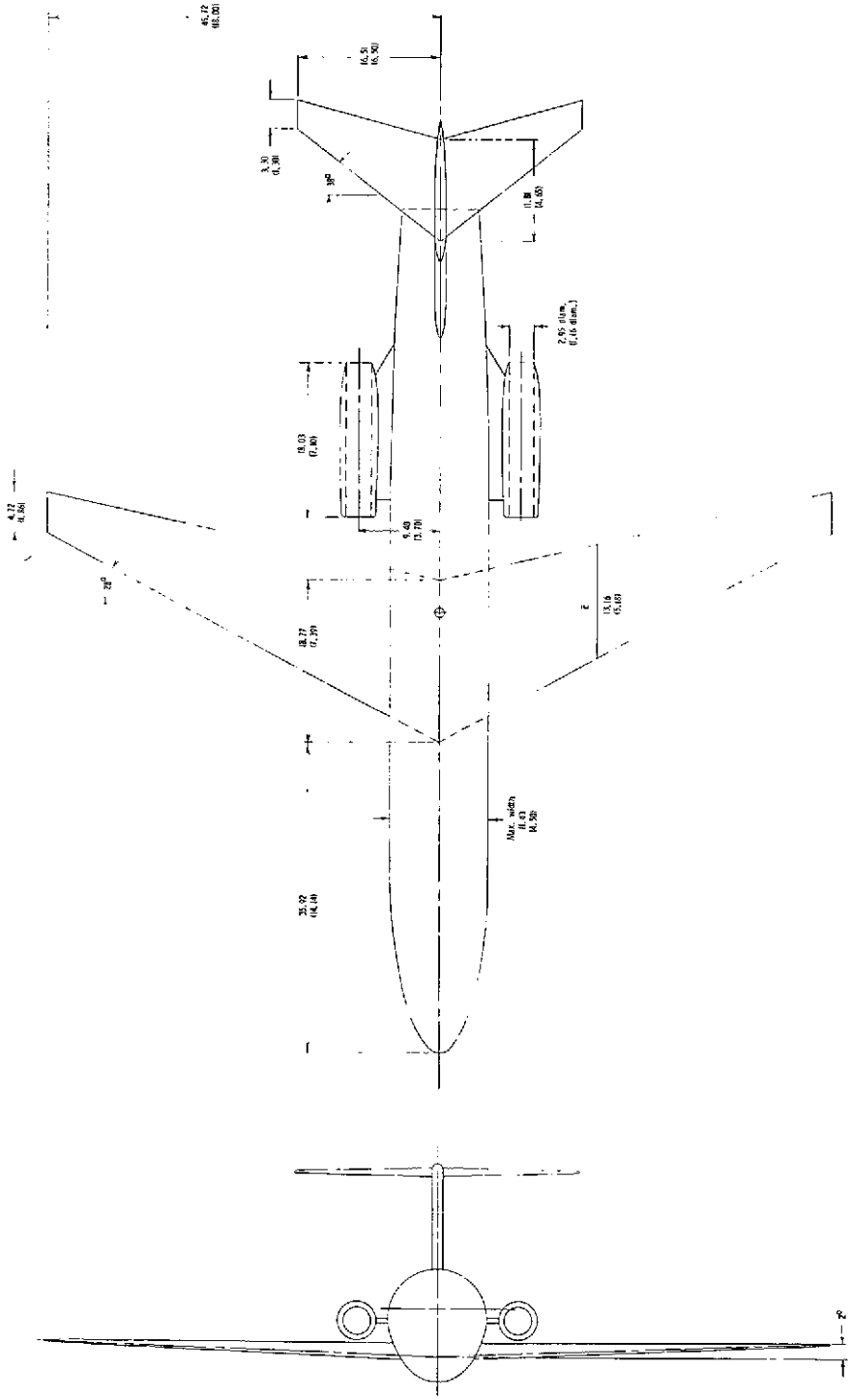

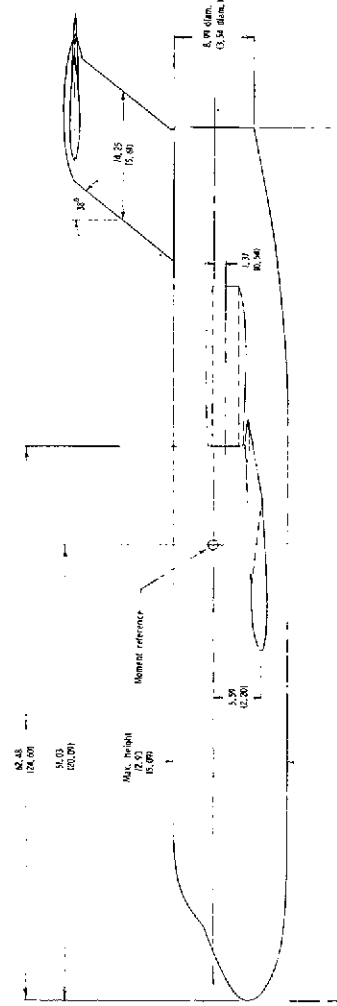

Figure 2.- Details of model. All linear dimensions are in centimeters (inches).

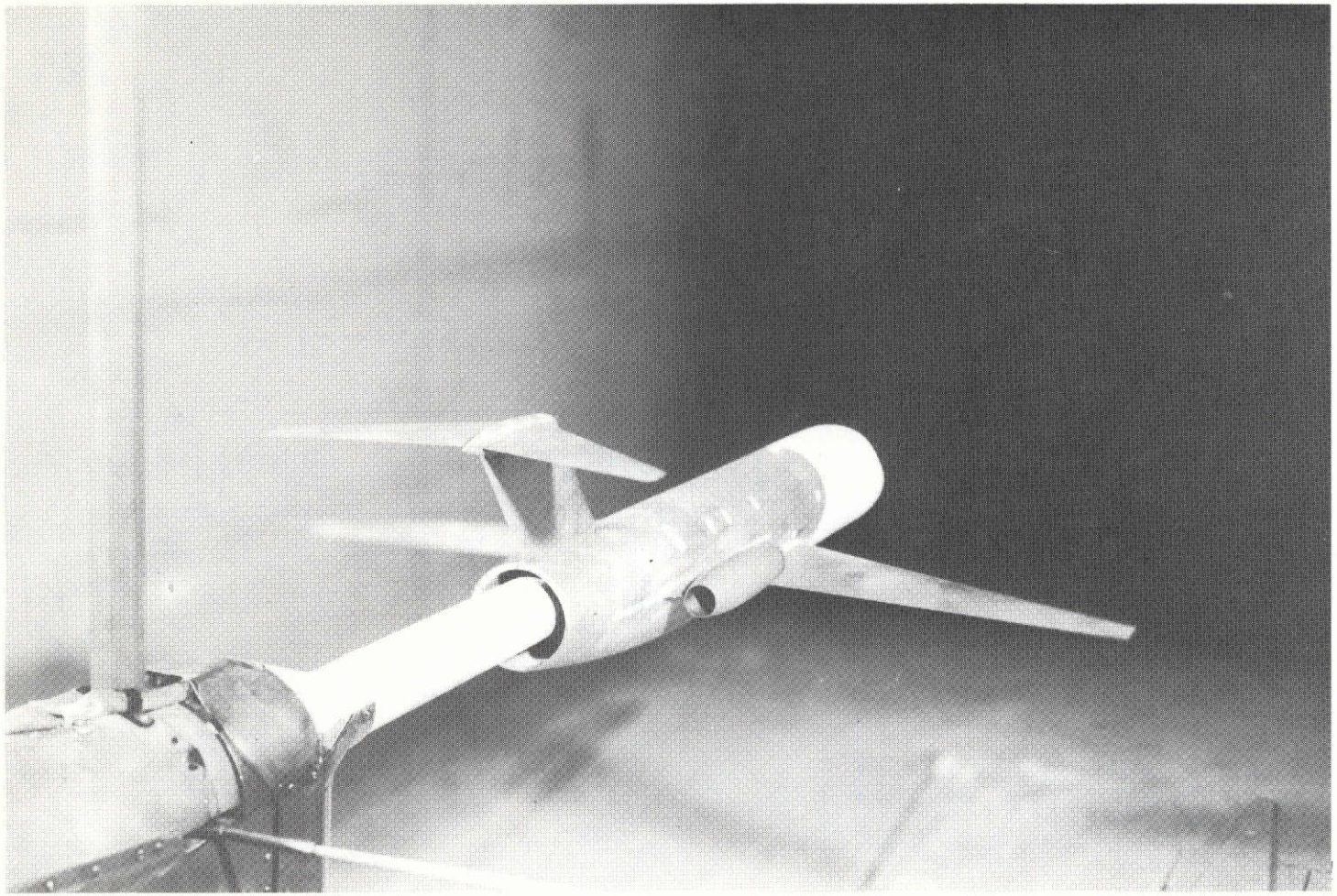

L-69-6648

Figure 3.- T-tail transport model mounted on forced-oscillation roll mechanism.

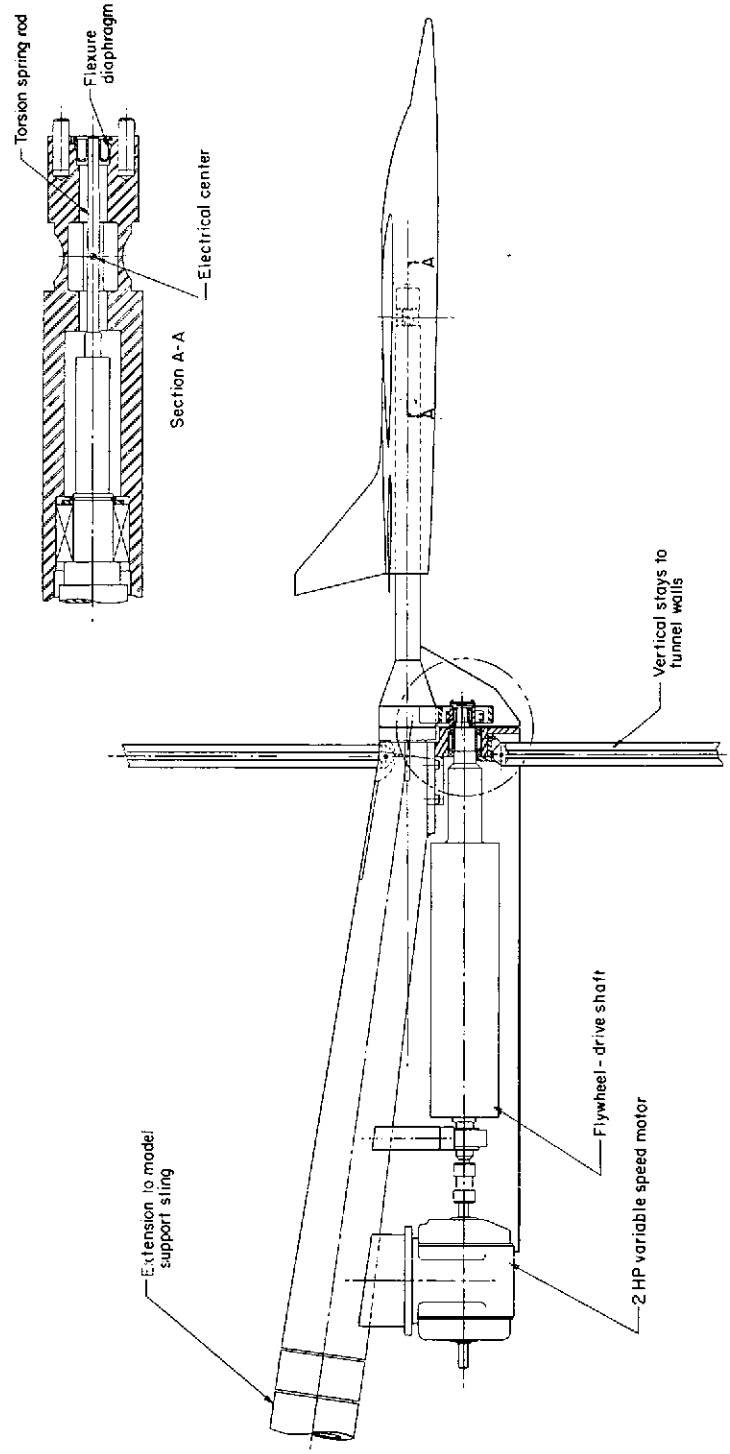

Figure 4.- Forced-oscillation roll mechanism.

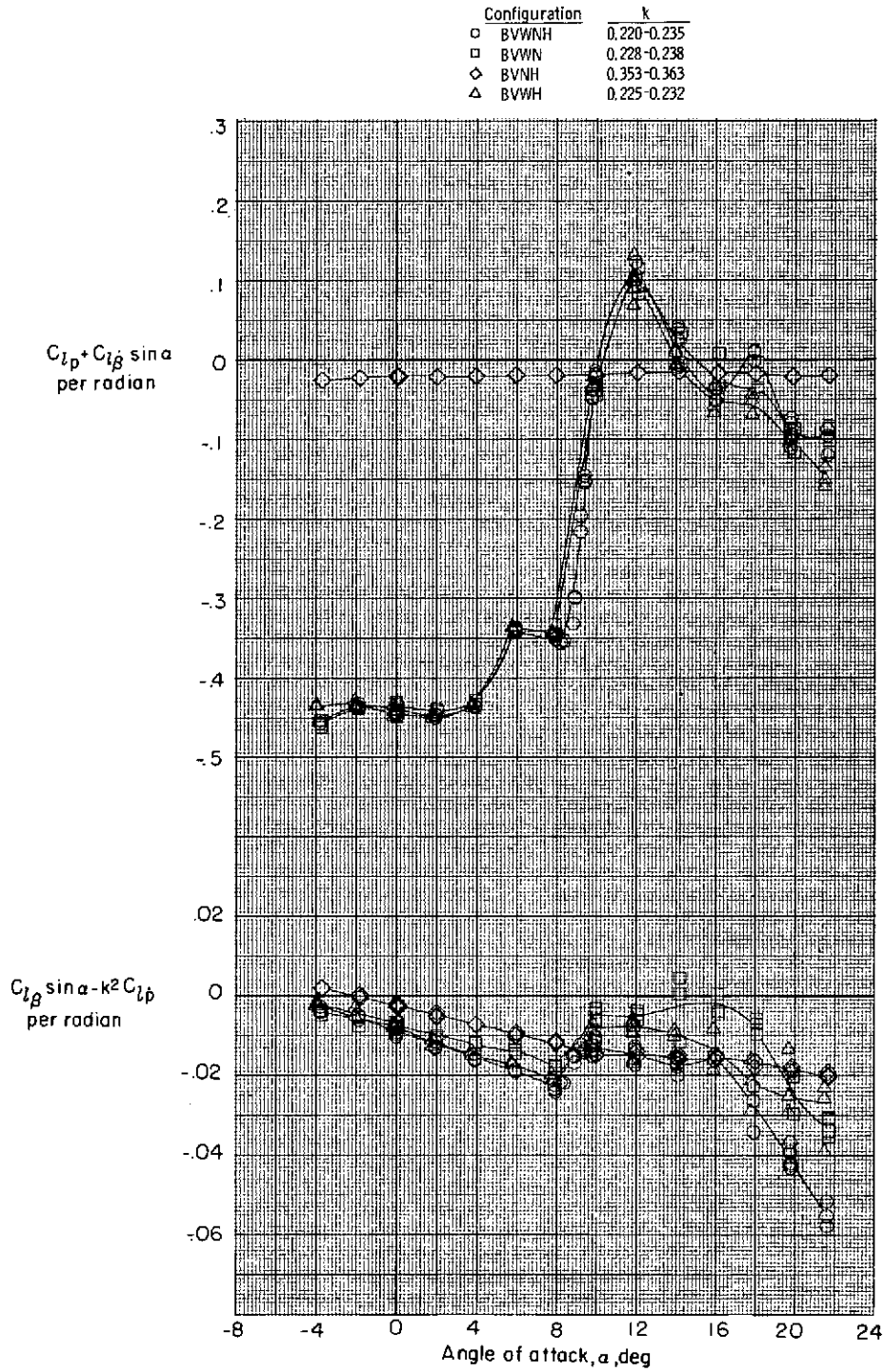

(a) M = 0.21.

Figure 5.- Effect of various configurations on damping-in-roll parameter and on rolling moment due to roll displacement parameter.

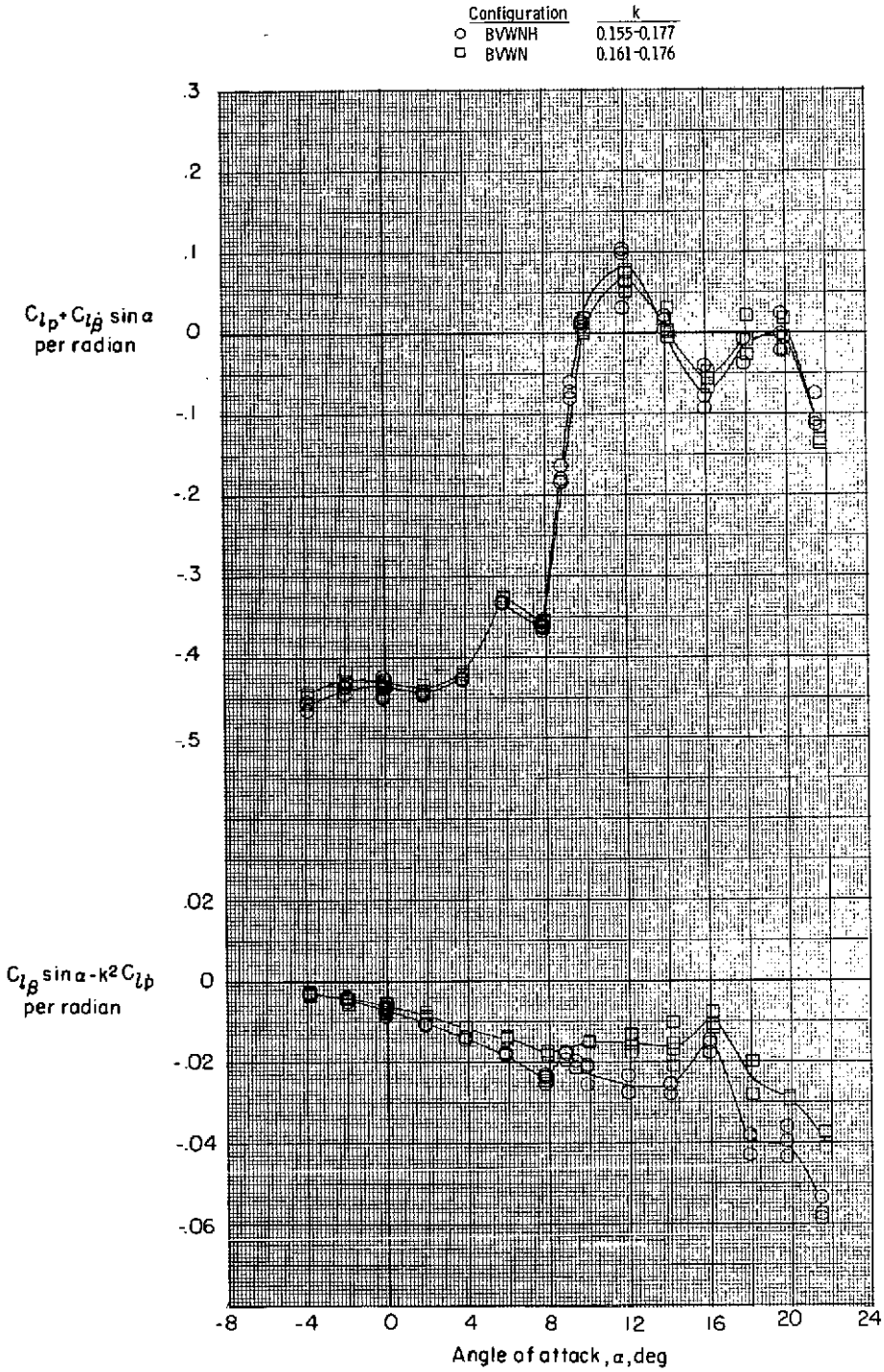

(b) M = 0.30.

Figure 5.- Continued.

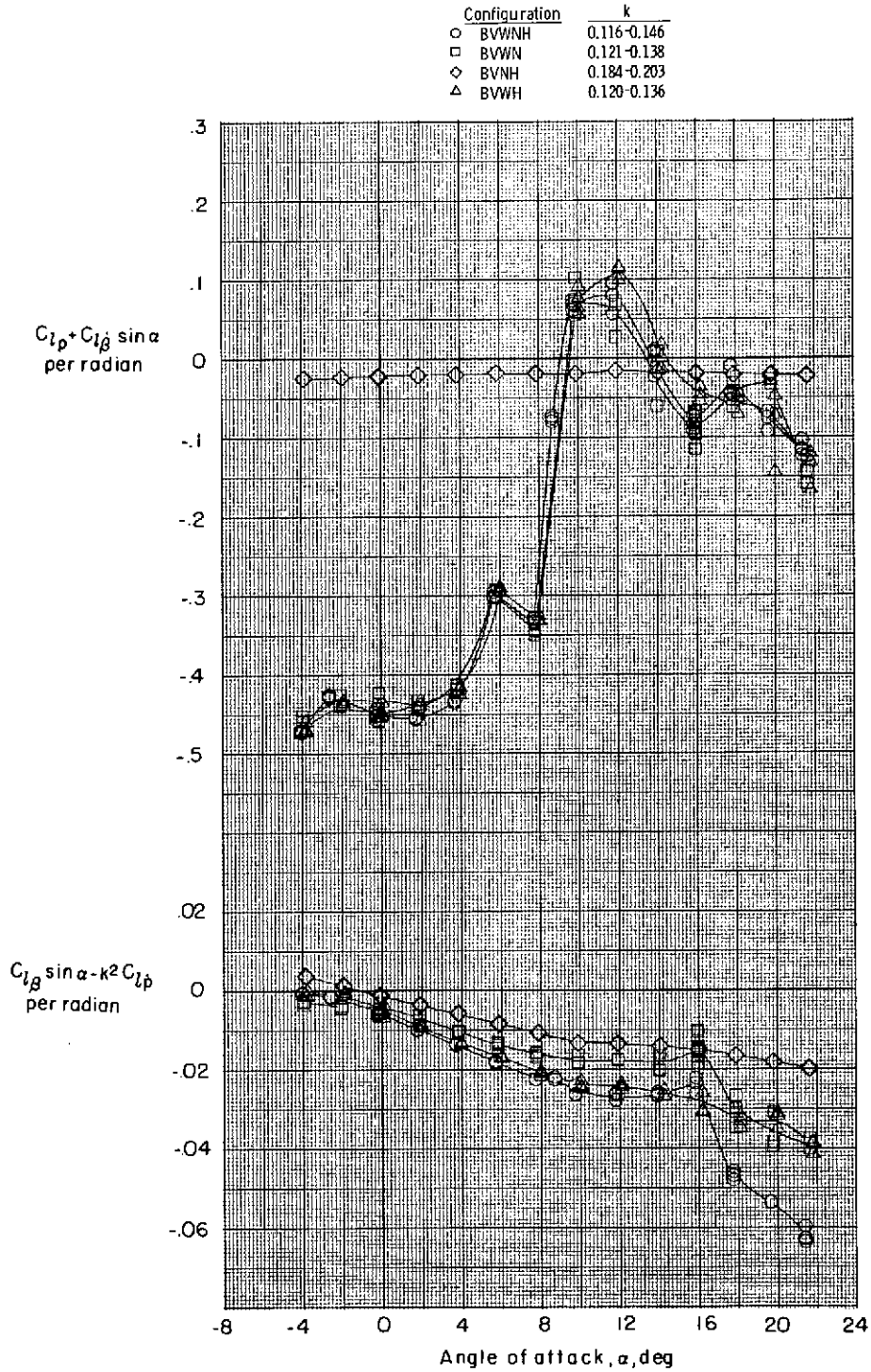

(c) M = 0.40.

Figure 5.- Continued.

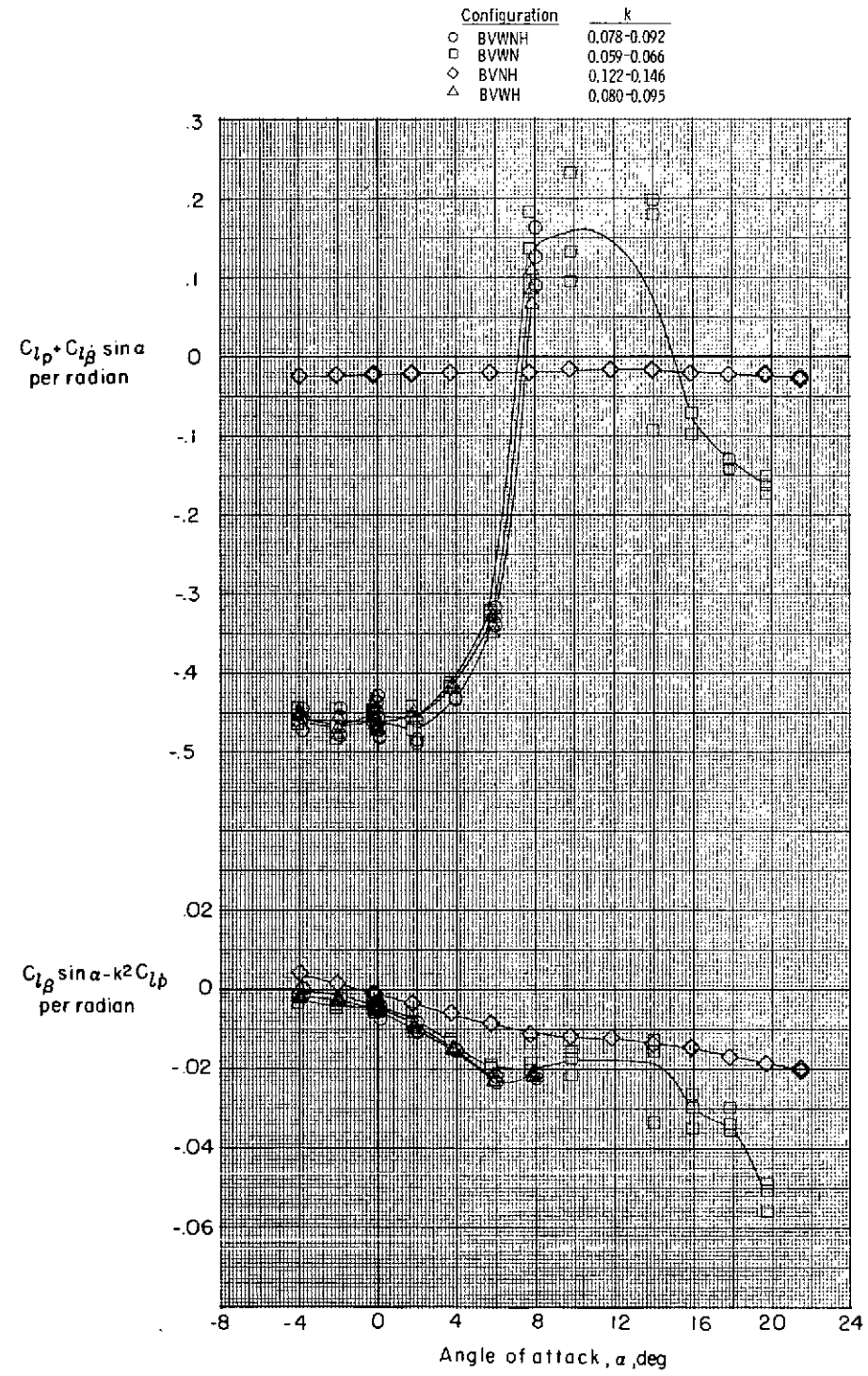

(d) M = 0.60.

Figure 5.- Continued.

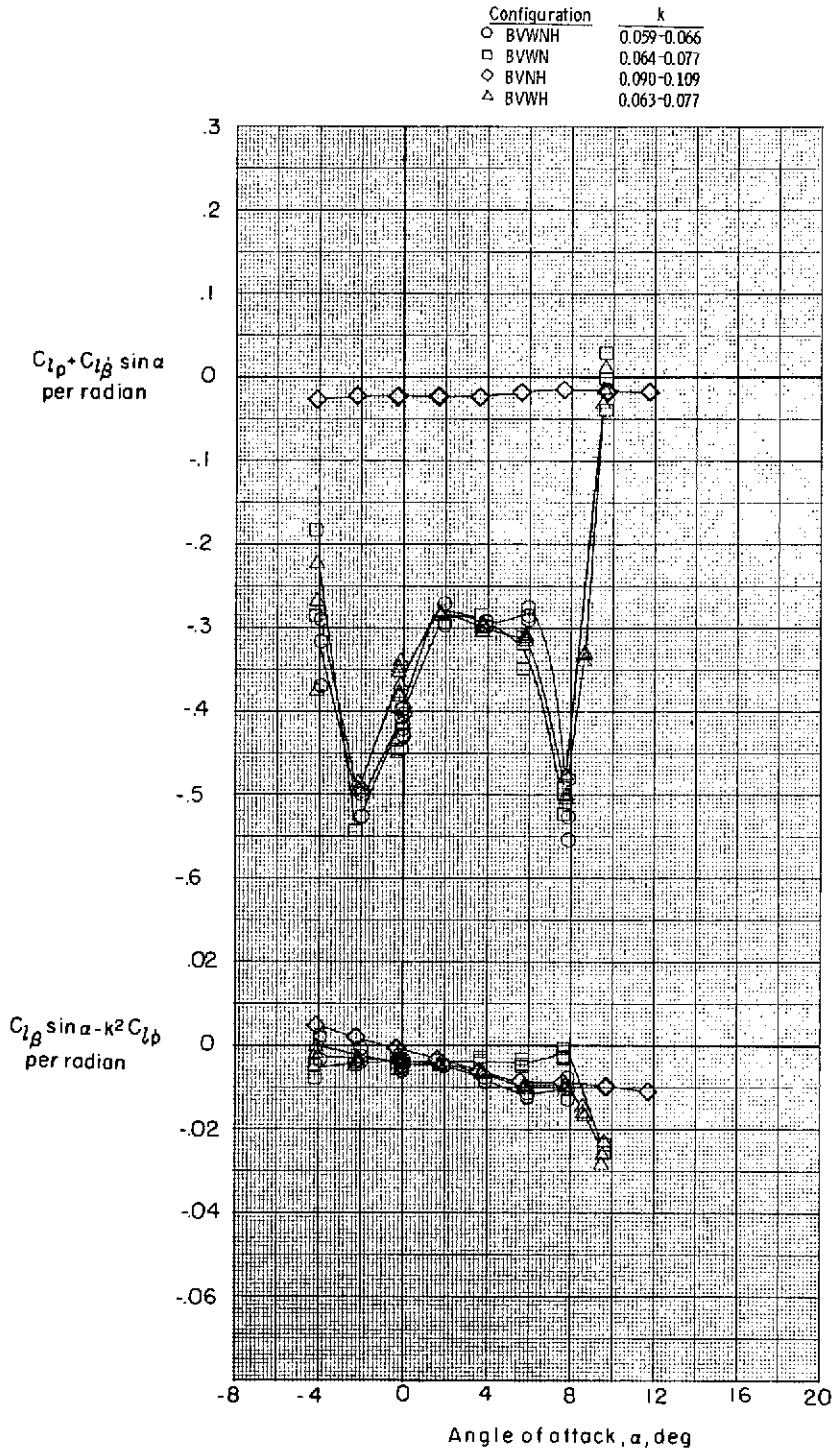

(e) M = 0.80.

Figure 5.- Concluded.

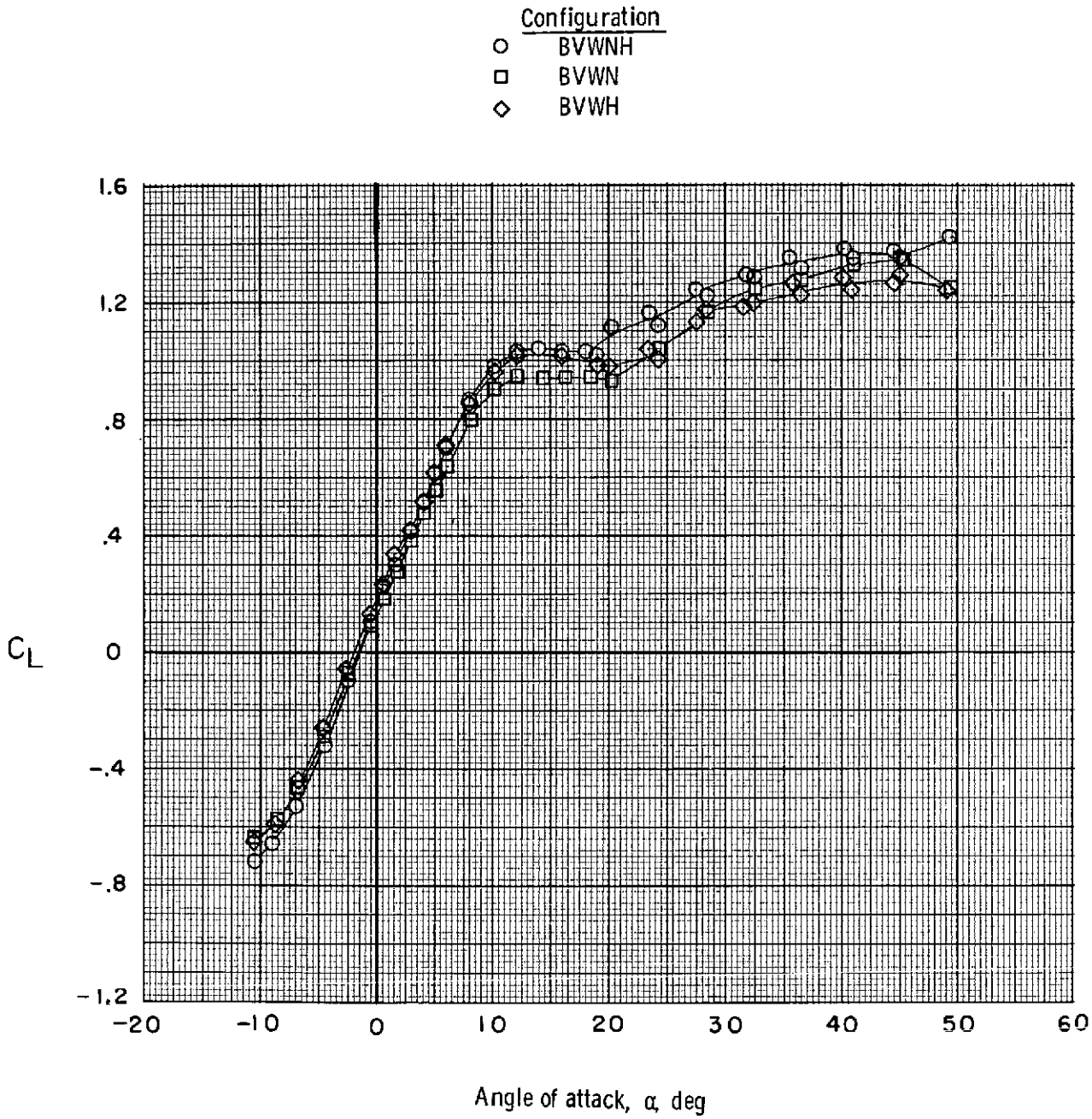

Figure 6.- Effect of various configurations on lift characteristics. M = 0.21; R = 0.78×10^6. (Data are from ref. 1.)

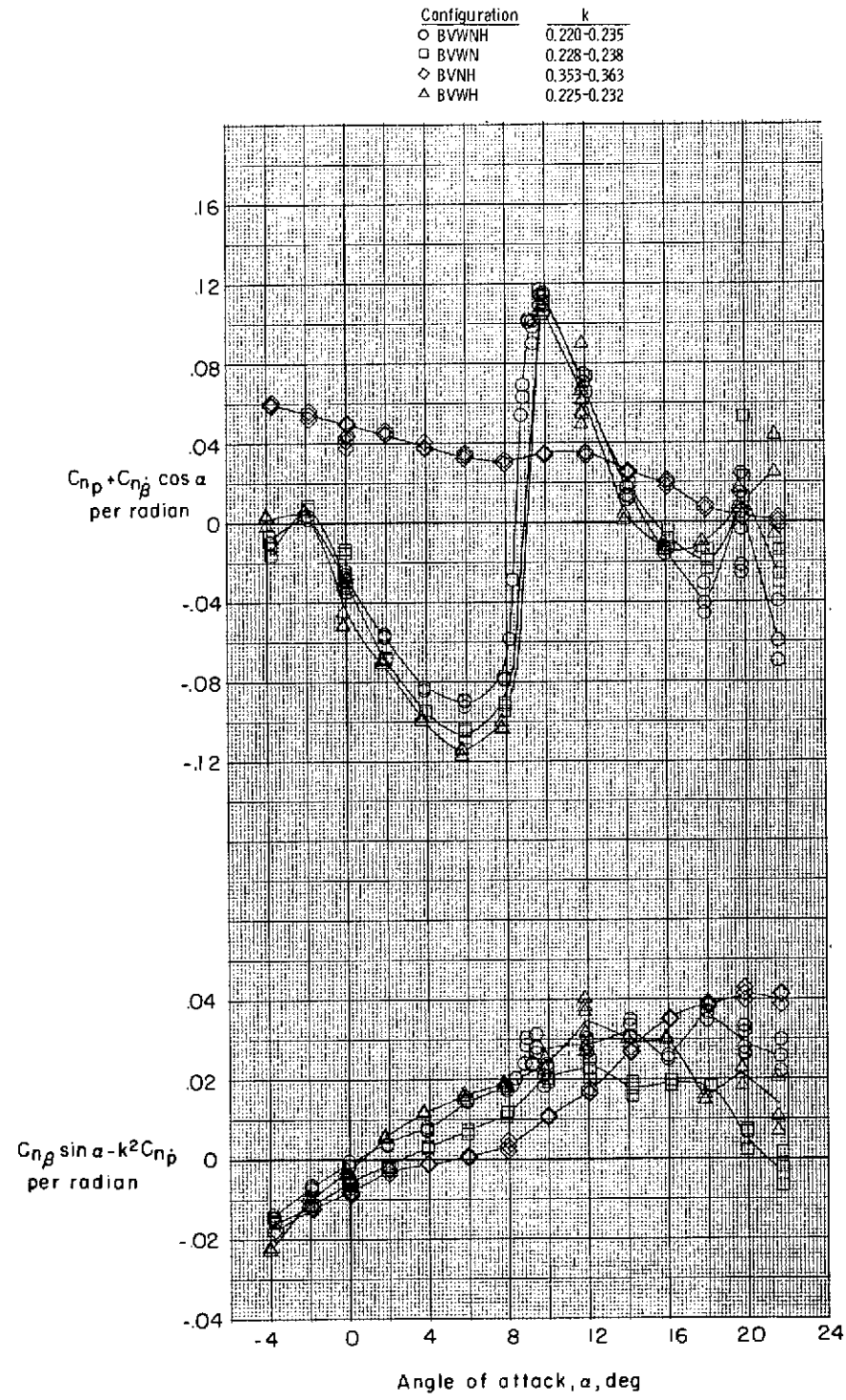

(a) M = 0.21.

Figure 7.- Effect of various configurations on yawing moment due to roll rate parameter and on yawing moment due to roll displacement parameter.

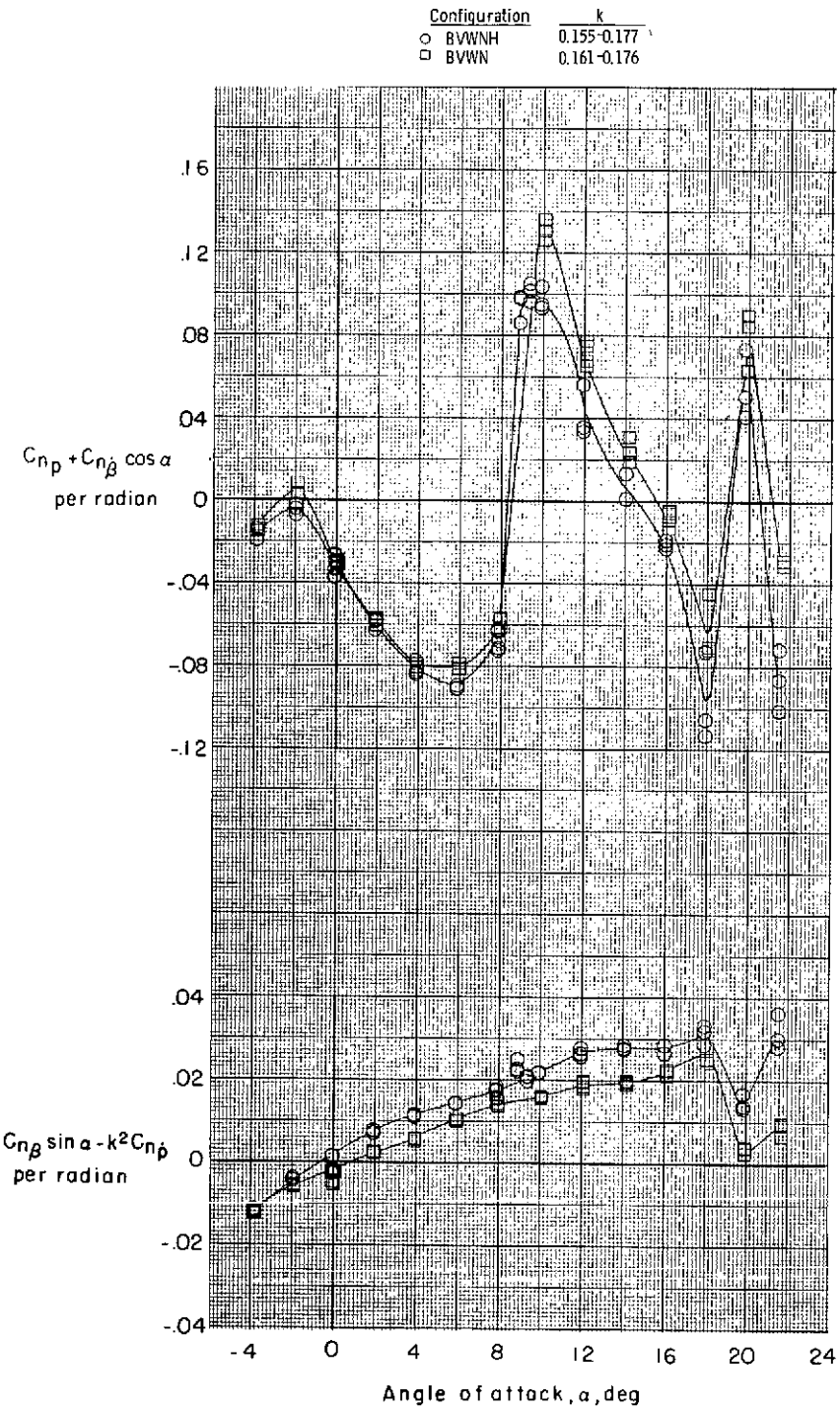

(b) M = 0.30.

Figure 7.- Continued.

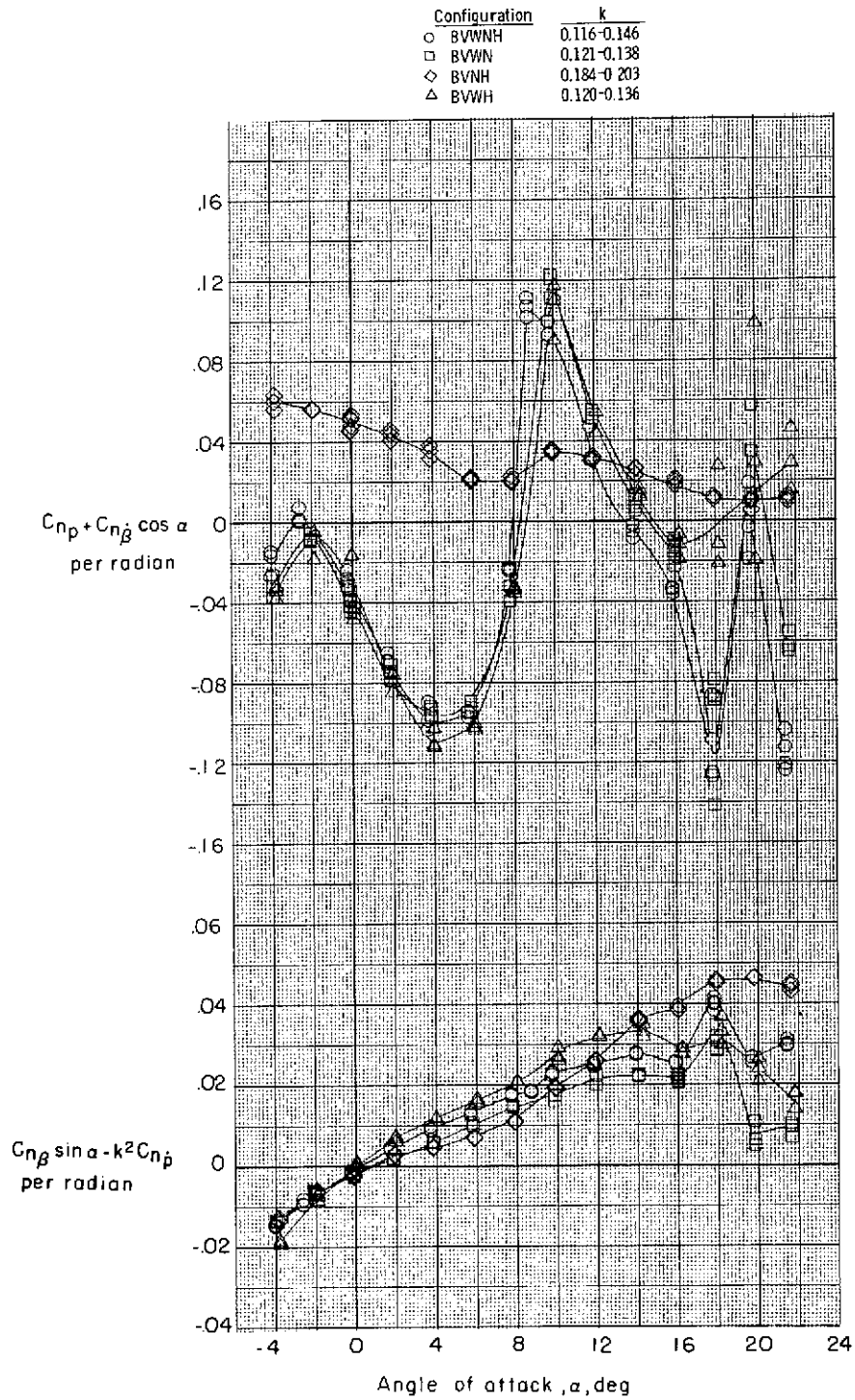

(c) M = 0.40.

Figure 7.- Continued.

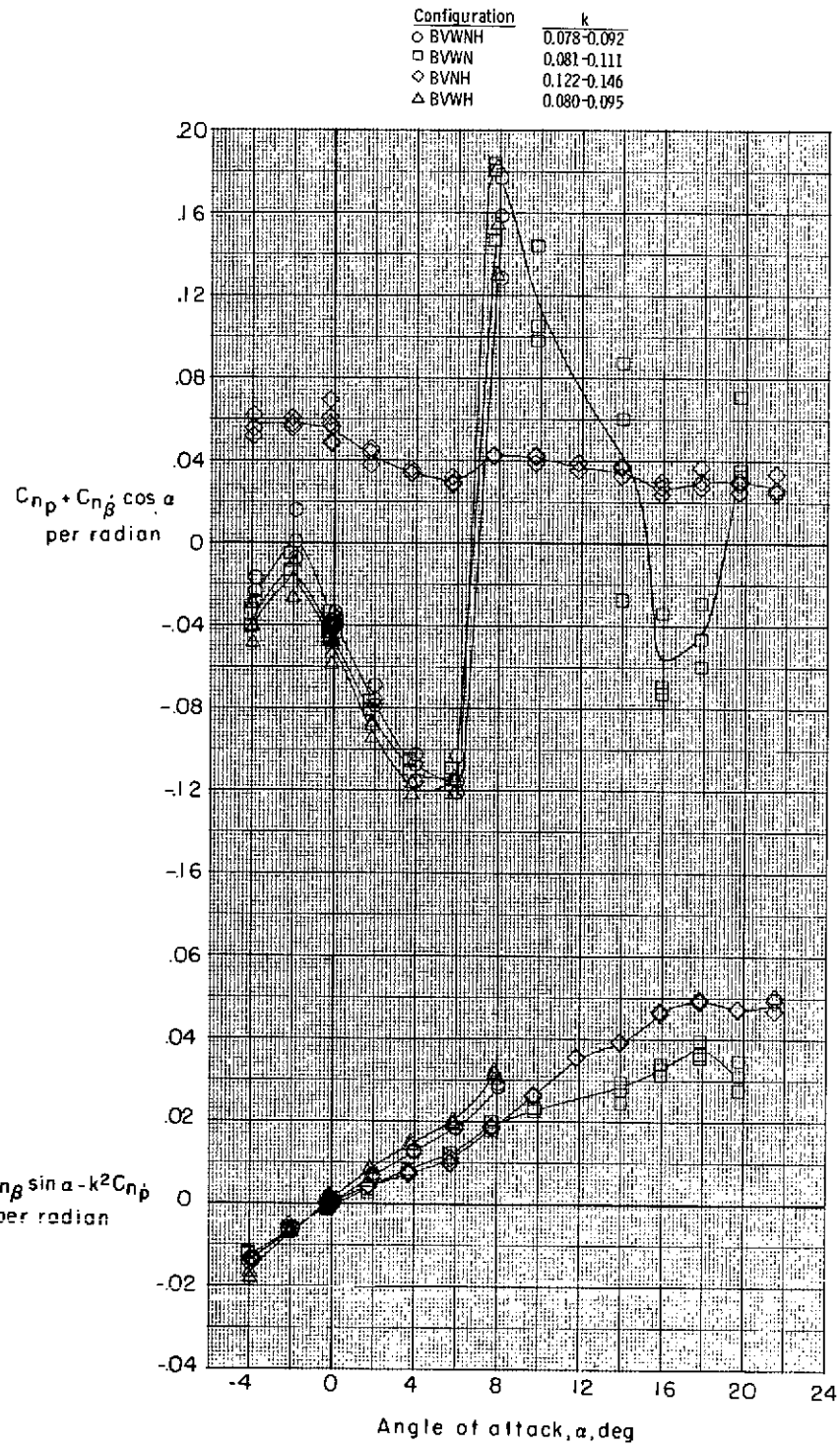

(d) M = 0.60.

Figure 7.- Continued.

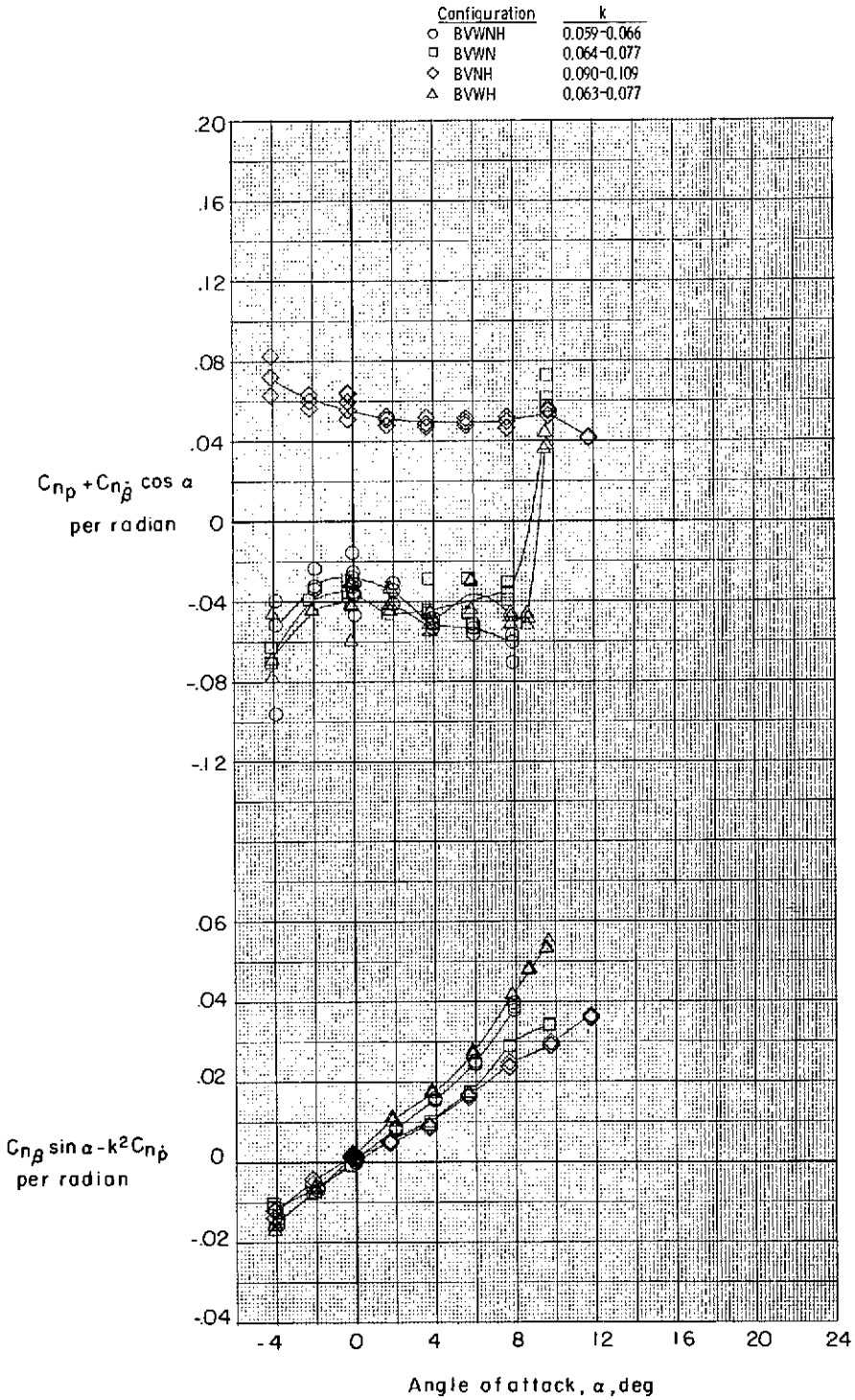

(e) M = 0.80.

Figure 7.- Concluded.

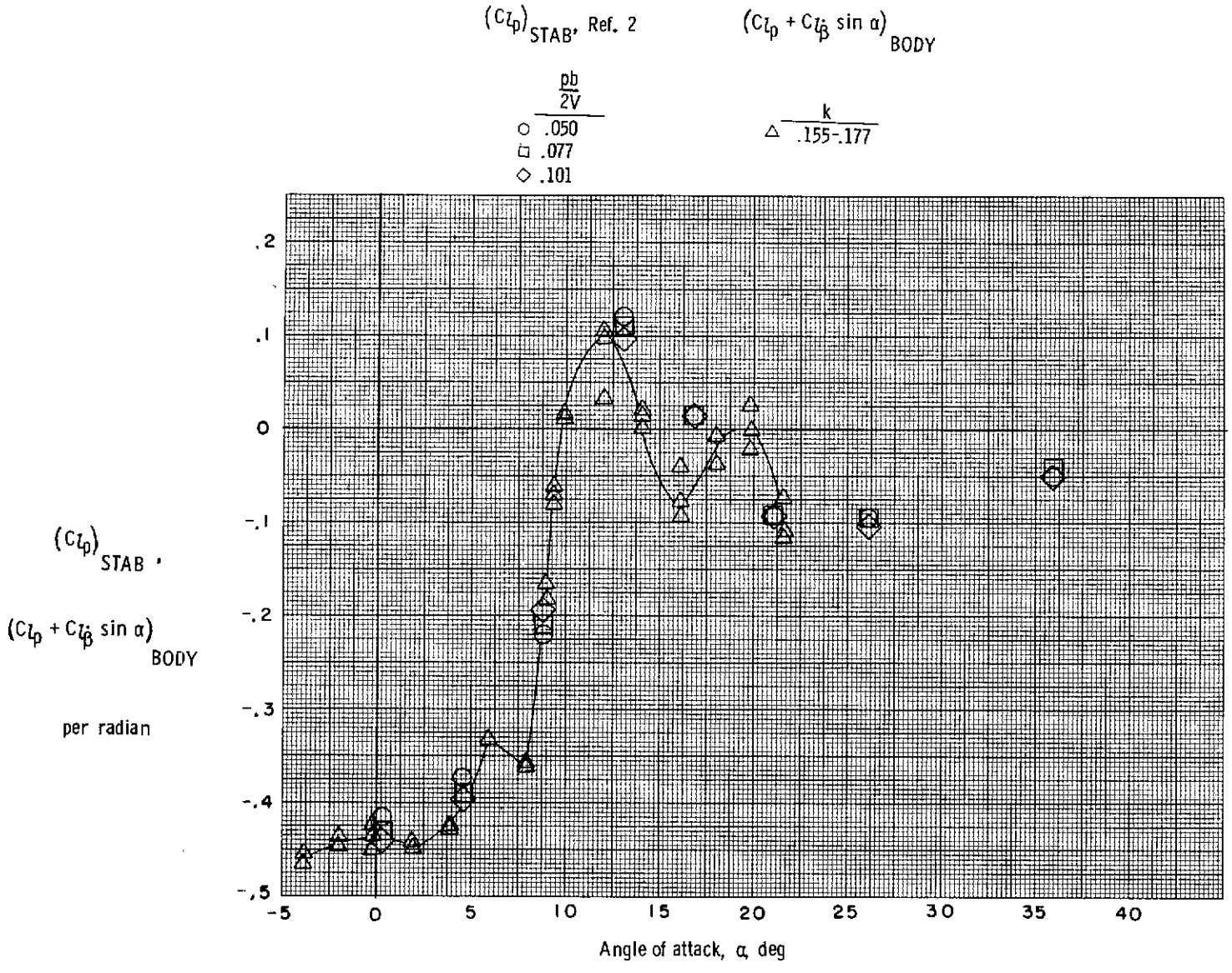

Figure 8.- Body-axis forced-oscillation roll damping parameter and stability-axis forced steady-state roll damping coefficient for basic configuration (BVWNH) at M = 0.30.

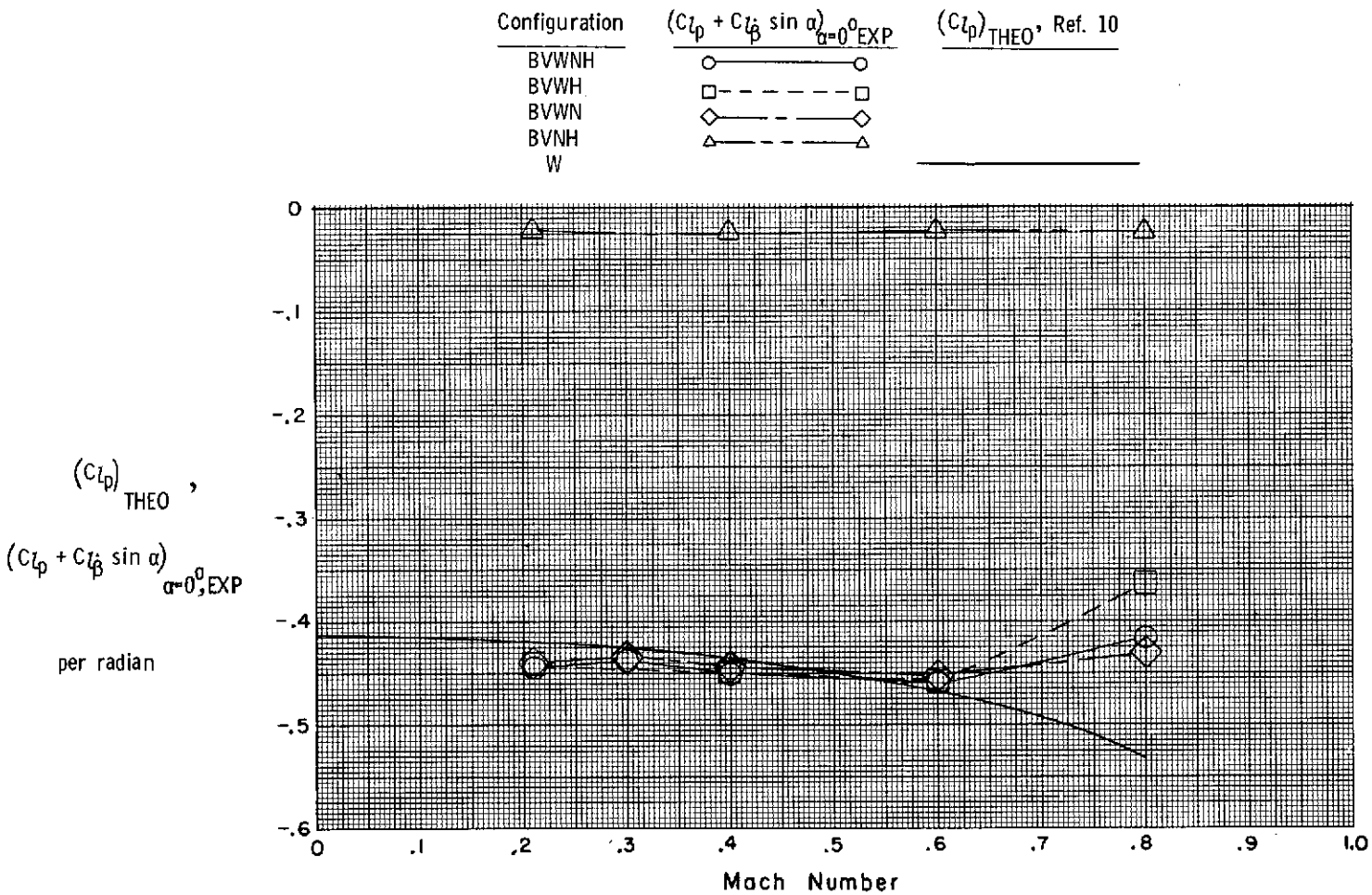

Figure 9.- Experimental results for various configurations at $\alpha = 0^0$ and theoretical estimates for wing alone.